Trim-coupled Flap analysis of a Rotor Blade in Forward Flight

Kumar Ravichandran

September 29, 2008

Department of Aerospace Engineering,
University of Maryland, College Park

Abstract

The flap-only response of an elastic rotor blade in forward flight was computed. A linear, quasi-steady aerodynamic model with only circulatory loads was considered.The blade displacements were used to determine hub and hence vehicle loads, which were then used to trim the rotor. theEffects of fuselage, tail rotor, interference etc. were ignored. The Finite Element Method, in both time and space, was the basis for the analysis.

Introduction

The goal of the exercise is to achieve a steady trim condition in forward flight i.e. the average loads generated by the rotor over a certain time period (naturally that corresponding to one rotor revolution) must balance those produced by the rest of the vehicle over every cycle.This implies the rotor motion must be periodic and must include feedback relating to the generated loads, so that the helicopter is kept in equilibrium. This is called ‘coupled trim’, because the flapping and vehicle equilibrium are solved concurrently.

Here, an initial rigid trim analysis was performed for specified flight conditions and thrust level. This is useful because in most cases, the final steady trimmed state is quite close to the rigid trimmed state, due to small flapping deflections.The rigid trim control settings were used to determine the steady rotor response.This was used to estimate the steady forces and moments, which awere fed into the trim equations. Depending on the magnitude of the trim residues, the control settings were advanced using a simple linear Jacobian.This process is continued until the trim equations are satisfied within a desired margin.The schematic for the complete analysis is given in fig. 1

1 Rigid Trim

The general set of trim equations for the equilibrium of the helicopter involves 13 variables (fuselage and taileffects will introduce 2 more, the fuselage side force and torque), namely :

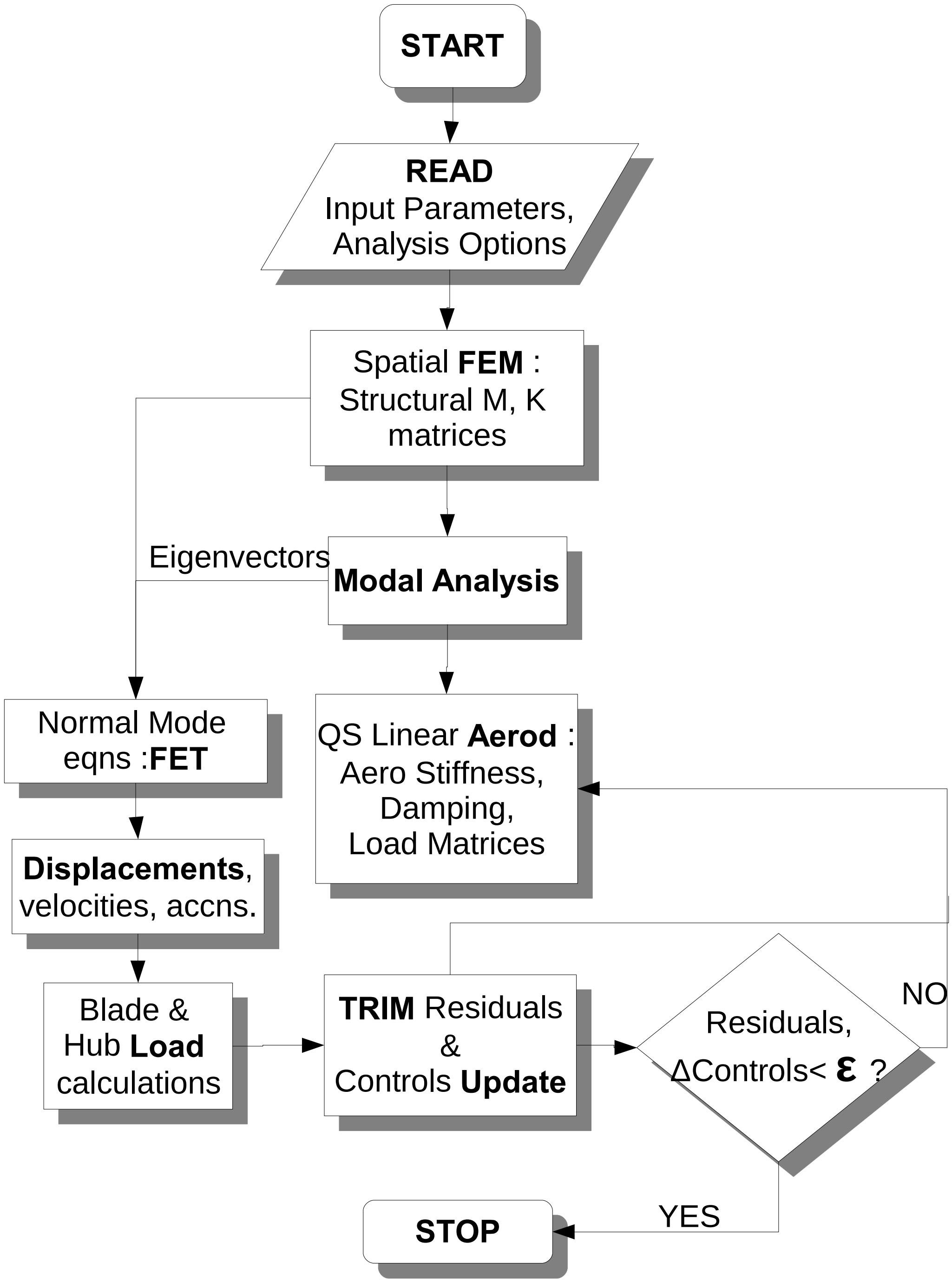

Figure 1: Process Flow diagram of Rotor Flap Analysis

α_S	− angle of attack/longitudinal shaft tilt
φ_S	− lateral shaft tilt
$\beta_0, \beta_{1c}, \beta_{1s}$	− Components of flap
T, H_{TPP}, Y_{TPP}	− Thrust, Drag and Side forces w.r.t Tip Path Plane
λ, λ_{TPP}	− Inflow - absolute and w.r.t TPP
$\theta_0, \theta_{1c}, \theta_{1s}$	− Components of blade pitch

The basic 6 trim equations (3 forces, Rolling and Pitching moments, and uniform inflow) are :

$$T \cos\alpha_S \cos\varphi_S + H \sin\alpha_S - Y \sin\varphi_S - W - D \sin\theta_{FP} = 0 \quad (1.1)$$

$$H \cos\alpha_S - T \sin\alpha_S \cos\varphi_S + D \sin\theta_{FP} = 0 \quad (1.2)$$

$$Y \cos\varphi_S + T \cos\alpha_S \sin\varphi_S = 0 \quad (1.3)$$

$$M_y - W(x_{cg} \cos\alpha_S - h \sin\alpha_S) - D(x_{cg} \sin(\alpha_S + \theta_{FP}) + h \cos(\alpha_S + \theta_{FP})) = 0 \quad (1.4)$$

$$M_x + W(h \sin\varphi_S - y_{cg} \cos\varphi_S) = 0 \quad (1.5)$$

$$\lambda_{TPP} = \mu \tan(\alpha_S + \beta_{1c} + \theta_{FP}) + \frac{K_f C_T}{2\sqrt{(\mu^2 + \lambda^2)}} \quad (1.6)$$

where T, H, Y, M_x, M_y are the rotor forces and the 2 moments of interest. D is the fuselage drag calculated using an equivalent flat plate area ($D = 1/2\rho V^2 f$); x_{cg}, y_{cg} are the offsets of the vehicle c.g. from the hub center; θ_{FP} is the flight path angle. The above are also checked as part of vehicle trim every revolution.

Also,

$$\lambda = \lambda_{TPP} \cos\beta_{1c} - \mu \sin\beta_{1c} \quad (1.7)$$

Assuming that the pitch distribution across azimuth ψ and radial location x is :

$$\theta(\psi, x) = \theta_0 + \theta_{tw} \frac{x}{R} + \theta_{1c} \cos\psi + \theta_{1s} \sin\psi \quad (1.8)$$

we can solve the flapping equation (Eqn. 1.9) in β, the flapping angle relative to the plane of the hub, assuming that $\beta = \beta_0 + \beta_{1c}\cos\psi + \beta_{1s}\sin\psi$. Here ν_β, $\nu_{\beta 0}$ are the rotating and non-rotating flap frequencies (/rev) and $\overline{M}_\beta$ is the aerodynamic flapping moment, related to the in-plane and normal velocities U_T, U_P ..

$$\ddot{\beta} + \nu_\beta^2\beta = \gamma\overline{M}_\beta + \nu_{\beta 0}^2\beta_P \tag{1.9}$$

$$\overline{M}_\beta = \frac{1}{2}\int_0^1 x\left[\left(\frac{U_T}{\Omega R}\right)^2\theta_0 - \frac{U_T}{\Omega R}\frac{U_P}{\Omega R}\right]dx$$

This expressions for the flap angles and pitch controls,6 in all. That makes 13 equations,which are solved iteratively for the given vehicle and flight conditions to give the initial trim state. To facilitate the non-linear rigid trim calculation, the above equations may be linearized to get a quick converged solution.

In the present analysis, N_b identical blades are assumed with specified pretwist θ_{tw} and precone β_p. The blade c.g. is assumed to lie on its elastic axis.

2 Structural Model

The modeling, non-dimensionalization scheme and notation are the same as that in the UMARC manual.

2.1 Blade Coordinate Systems

The different frames of reference that are of interest are :

1. fixed to the hub - coordinates (X_H, Y_H, Z_H) and unit vectors ($\hat{I}_H$, $\hat{J}_H$, $\hat{K}_H$)
2. rotating w.r.t the hub - coordinates (X, Y, Z) and unit vectors ($\hat{I}$, $\hat{J}$, $\hat{K}$)
3. undeformed blade system - coordinates (x, y, z) and unit vectors ($\hat{i}$, $\hat{j}$, $\hat{k}$)
4. deformed blade system - coordinates (ξ, η, ζ) and unit vectors ($\hat{i}_\xi$, $\hat{j}_\eta$, $\hat{k}_\zeta$)

$(\hat{I}, \hat{J}, \hat{K})$ is simply displaced from $(\hat{I}_H, \hat{J}_H, \hat{K}_H)$ by an angle $\psi = \Omega t$. $(\hat{i}, \hat{j}, \hat{k})$ is at an angle equal to β_p, the precone angle, w.r.t $(\hat{I}_H, \hat{J}_H, \hat{K}_H)$. The crucial transformation is that between the undeformed and deformed blade coordinates.

The rotor blades are modeled as isotropic Euler-Bernoulli beams i.e. slender beams with transverse shear stresses neglected in comparison to the longitudinal stresses, small deformations and plane cross-sections remaining plane and normal to the elastic axis at all times. Under these assumptions, it may be shown that

$$\begin{Bmatrix} \hat{i}_\xi \\ \hat{j}_\eta \\ \hat{k}_\zeta \end{Bmatrix} = \begin{bmatrix} 1 - \frac{w'^2}{2} & 0 & w' \\ -w' \sin\theta_0 & \cos\theta_0 & (1 - \frac{w'^2}{2})\sin\theta_0 \\ -w' \cos\theta_0 & -\sin\theta_0 & (1 - \frac{w'^2}{2})\cos\theta_0 \end{bmatrix} \begin{Bmatrix} \hat{i} \\ \hat{j} \\ \hat{k} \end{Bmatrix} = \boldsymbol{T_{DU}} \begin{Bmatrix} \hat{i} \\ \hat{j} \\ \hat{k} \end{Bmatrix} \tag{2.1}$$

where w' denotes $\partial w/\partial r$ and θ_0 is the local pitch in this flap-only case, given by Eqn. 1.8.

2.2 Variational principle and FEM

Hamilton's variational principle is expressed as

$$\delta\Pi = \int_{t_1}^{t_2} (\delta U - \delta T - \delta W)dt = 0 \tag{2.2}$$

where $\delta U, \delta T, \delta W$ are virtual variations in strain energy, kinetic energy and external virtual work. The above may be seen as a sum of individual virtual energy expressions for the blades :

$$\delta\Pi_b = \int_{\psi_i}^{\psi_f} \sum_{i=1}^{N_r} (\delta U_i - \delta T_i - \delta W_i)dt = 0 \tag{2.3}$$

N_r is the number of spatial finite elements in the blade. The blade is discretized into spatial elements each with 4 degrees of freedom over 2 nodes (displacement and slope at each node). Ensuring continuity of these degrees of freedom gives us the transformation from nodal displacements to displacement w at any location in an element (length l) :

$$w = \left[2s^3 - 3s^2 + 1 \quad s^3 - 2s^2 + s \quad -2s^3 + 3s^2 \quad s^3 - s^2\right] \begin{Bmatrix} w_1 \\ l_i w_1' \\ w_2 \\ l_i w_2' \end{Bmatrix} \tag{2.4}$$

$$= \left[H_1 \; H_2 \; H_3 \; H_4\right] \begin{Bmatrix} w_1 \\ l_i w_1' \\ w_2 \\ l_i w_2' \end{Bmatrix} \tag{2.5}$$

$$= \boldsymbol{Hq} \tag{2.6}$$

where the Hs are called the shape functions, and local element coordinate $s = x/l$ goes from 0 to 1. The elemental energy variation then becomes

$$\delta\Pi_i = \delta\boldsymbol{q}_i^T(\boldsymbol{M}_b\ddot{\boldsymbol{q}} + \boldsymbol{C}_b\dot{\boldsymbol{q}} + \boldsymbol{K}_b\boldsymbol{q} - \boldsymbol{F}_b)_i - \delta\boldsymbol{W}_i \tag{2.7}$$

and the elemental mass, damping, stiffness and load matrices are (m is mass per unit length; m_0 is the reference value) :

$$(\boldsymbol{M}_b)_i = \int_0^1 m\boldsymbol{H}^T\boldsymbol{H}ds \tag{2.8}$$

$$(\boldsymbol{C}_b)_i = 0 \tag{2.9}$$

$$(\boldsymbol{K}_b)_i = \int_0^1 m[F_A\boldsymbol{H}'^T\boldsymbol{H}' + (EI_y\sin^2\theta_0 + EI_z\cos^2\theta_0)\boldsymbol{H}''^T\boldsymbol{H}'']ds \tag{2.10}$$

$$(\boldsymbol{F}_b)_i = -\int_0^1 m\Omega^2\beta_p\boldsymbol{H}^T ds \tag{2.11}$$

3 Aerodynamic Model

The quasi-steady aerodynamic assumption means that the aerodynamic loads are functions purely of the instantaneous blade section angle of attack. The incident flow velocity on the deformed blade is sufficient to calculate the finite element aerodynamic stiffness, damping and load matrices.

3.1 Velocities

Basic Blade Element analysis yields the resultant velocity in the deformed frame to be

$$\overline{V} = U_R \hat{i}_\xi + U_T \hat{j}_\eta + U_P \hat{k}_\zeta \tag{3.1}$$

where the non-dimensional velocity components are

$$\begin{aligned} u_R = \frac{U_R}{\Omega R} &= (-\mu\cos\psi + \lambda\beta_p - \eta_r\cos\theta_0) + (\mu\cos\psi\beta_p + \lambda)w^{0} \\ &\quad -(\eta_r\sin\theta_0)\dot{w}^{0} + \dot{w}w^{0} + \frac{1}{2}\mu\cos\psi w^{02} \end{aligned} \tag{3.2}$$

$$\begin{aligned} u_T = \frac{U_T}{\Omega R} &= [\cos\theta_0(x + \mu\sin\psi) + \sin\theta_0(\lambda + \mu\cos\psi\beta_p)] - (\beta_p\cos\theta_0)w \\ &\quad +(\sin\theta_0)\dot{w} + (\mu\cos\psi\sin\theta_0)w^{0} \end{aligned} \tag{3.3}$$

$$\begin{aligned} u_P = \frac{U_P}{\Omega R} &= [-\sin\theta_0(x + \mu\sin\psi) + \cos\theta_0(\lambda + \mu\cos\psi\beta_p) + \eta_r(\dot{\theta}_0 + \beta_p)] \\ &\quad +(\beta_p\sin\theta_0)w + (\cos\theta_0)\dot{w} + (\mu\cos\psi\cos\theta_0 + \eta_r)w^{0} \end{aligned} \tag{3.4}$$

where η_r is the location of the three-quarter chord line ahead of the elastic axis ($\eta = 0$), non-dimensionalized w.r.t R.

3.2 Quasi-steady Loads

The aerodynamic coefficients are expressed as :

$$C_l = c_0 + c_1\alpha\ ; \quad C_d = d_0 + d_1|\alpha| + d_2\alpha^2\ ; \quad C_m = c_{mac} + f_1\alpha \tag{3.5}$$

The deformed frame loads per unit length are given as (force dimension $\sim m_0\Omega^2 R$, moments $\sim m_0\Omega^2 R^2$)

$$\overline{L}_u = \frac{\gamma}{6a}(-d_0 u_R u_T) \tag{3.6}$$

$$\overline{L}_v = \frac{\gamma}{6a}(-d_0 u_T^2 - (c_0 u_P - d_1|u_P|)u_T + (c_1 - d_2)u_P^2) \tag{3.7}$$

$$\overline{L}_w = \frac{\gamma}{6a}(c_0 u_T^2 - (c_1 + d_0)u_T u_P + d_1|u_P|u_P) \tag{3.8}$$

$$\overline{M}_\varphi = \frac{\gamma}{6a}(\frac{c}{R}(c_{mac}(u_T^2 + u_P^2) - f_1 u_T u_P)) - e_d\overline{L}_w \tag{3.9}$$

Here, γ is the Lock number, a is reference ç and e_d is the chordwise offset of the aerodynamic center w.r.t the elastic axis.

Transforming the loads to the undeformed blade frame,

$$\begin{bmatrix} L_u^A \\ L_v^A \\ L_w^A \end{bmatrix} = \boldsymbol{T_{DU}}^{-1} \begin{bmatrix} \overline{L}_u \\ \overline{L}_v \\ \overline{L}_w \end{bmatrix} \tag{3.10}$$

$$\begin{bmatrix} M_{\varphi u}^A \\ M_{\varphi v}^A \\ M_{\varphi w}^A \end{bmatrix} = \boldsymbol{T_{DU}}^{-1} \begin{bmatrix} \overline{M}_\varphi \\ 0 \\ 0 \end{bmatrix} \tag{3.11}$$

Writing the aerodynamic normal force as a sum of constant, linear and higher-order components,

$$L_w^A = L_w^A|_0 + (A_w w + A_w \dot{w} + A_{w^0} w^0) + (L_w^A)_{nl} \tag{3.12}$$

and the nonlinear part is linearized about the current trimmed response using a Taylor series approximation :

$$L_w^A|_{nl} = (L_w^A)_{nl}|_{w_0} + A_w^0|_{w_0}(w - w_0) + A_w^0|_{w_0}(\dot{w} - w_0) + A_{w^0}^0|_{w_0}(w^0 - w_0^0) \tag{3.13}$$

Then the blade virtual work for the ith element is obtained as

$$(\delta W_b)_i = \delta \boldsymbol{q}_i^T (\boldsymbol{C}_b^A \dot{\boldsymbol{q}} + \boldsymbol{K}_b^A \boldsymbol{q} + \boldsymbol{F}_b^A)_i \tag{3.14}$$

the element aerodynamic matrices being

$$(\boldsymbol{C}_b^A)_i = l_i \int_0^1 (A_w + A_w|_{w_0}) \boldsymbol{H}^T \boldsymbol{H} ds \tag{3.15}$$

$$(\boldsymbol{K}_b^A)_i = l_i \int_0^1 [(A_w + A_w^0|_{w_0}) \boldsymbol{H}^T \boldsymbol{H} + (A_w^0 + A_{w^0}^0|_{w_0}) \boldsymbol{H}^T \boldsymbol{H}^0] ds \tag{3.16}$$

$$(\boldsymbol{F}_b^A)_i = l_i \int_0^1 \boldsymbol{H}^T [L_w^A|_0 + (L_w^A)_{nl}|_{w_0} - A_w^0|_{w_0} w_0 - A_w^0|_{w_0} \dot{w}_0 - A_{w^0}^0|_{w_0} w_0^0] ds \tag{3.17}$$

Adding the aerodynamic and structural matrices, assembling the finite elements and imposing the boundary conditions, we get the blade equation of motion in the nodal degrees of freedom

$$\boldsymbol{M} \ddot{\boldsymbol{q}}_b + \boldsymbol{C}(\psi) \dot{\boldsymbol{q}}_b + \boldsymbol{K}(\psi) \boldsymbol{q}_b = \boldsymbol{F}(\psi) \tag{3.18}$$

Lets say the matrices are of size $N \times N$. For the case of a hingeless blade modeled with N_r spatial elements, the matrices are of size $2N_r \times 2N_r$.

4 Blade response

4.1 Modal Reduction

The flap-only case is mostly linear in the domain of operation, which allows us to write the response as a linear superposition of the natural modes, weighted with time-varying amplitudes, which are solved for from the reduced equation of motion Eqn. 3.18. It is also observed that the first few modes have a dominant effect on the final response,so only a few modes (N_m, say) are used to actually obtain the response.

Initially, the homogeneous equation of motion is solved to get the natural modes (and frequencies) of the system.

4.2 Finite Element in Time

Let $[\boldsymbol{\varphi}]_{N\times N_m}$ denote the matrix of N_m modes chosen. Then, the vector of nodal degrees of freedom across the blade at any azimuth, is given as

$$[\boldsymbol{q}_b]_{N\times 1}(\psi) = [\boldsymbol{\varphi}]_{N\times N_m}[\boldsymbol{\Xi}_b]_{N_m\times 1}(\psi) \tag{4.1}$$

The temporal coordinate Ξ is again approximated using Lagrange polynomials as shape functions in *time*. If an n_t order polynomial is used, then n+ 1 nodes per time element are needed.There is continuity between elements and periodicity between 2π cycles i.e. successive revolutionsHamilton's principle gives us then, from Eqn. 3.18 :

$$\int_0^{2\pi} \delta\boldsymbol{\Xi}_b^T(\overline{\boldsymbol{M}}\,\ddot{\boldsymbol{\Xi}}_b + \overline{\boldsymbol{C}}\,\dot{\boldsymbol{\Xi}}_b + \overline{\boldsymbol{K}}\boldsymbol{\Xi}_b - \overline{\boldsymbol{F}})d\psi = 0 \tag{4.2}$$

where $\overline{\boldsymbol{M}} = \boldsymbol{\varphi}^T\boldsymbol{M}\boldsymbol{\varphi}$, $\overline{\boldsymbol{C}} = \boldsymbol{\varphi}^T\boldsymbol{C}\boldsymbol{\varphi}$, $\overline{\boldsymbol{F}} = \boldsymbol{\varphi}^T\boldsymbol{F}$

Integrating by parts and using periodicity considerations, we have, for N_t time elements per revolution

$$\sum_{j=1}^{N_t}\int_{\psi_j}^{\psi_{j+1}} (\delta\dot{\boldsymbol{\Xi}}^T\overline{\boldsymbol{M}}\,\dot{\boldsymbol{\Xi}} + \delta\boldsymbol{\Xi}^T\overline{\boldsymbol{C}}\,\dot{\boldsymbol{\Xi}} + \delta\boldsymbol{\Xi}^T\overline{\boldsymbol{K}}\boldsymbol{\Xi} - \delta\boldsymbol{\Xi}^T\overline{\boldsymbol{F}}) = 0 \tag{4.3}$$

Transferring to nodal time coordinates $\boldsymbol{\xi}$ by means of temporal shape functions $\boldsymbol{H}_t$, we have

$$[\boldsymbol{\Xi}_j]_{N_m\times 1}(\psi) = [\boldsymbol{H}_t]_{N_m\times(N_m\times(n_t+1))}(s)[\boldsymbol{\xi}_j]_{(N_m\times(n_t+1))\times 1}$$

s going from 0 to 1.

The shape function matrix $\boldsymbol{H}_t$ is given by

$$\boldsymbol{H}_t = [H_{t_1}\boldsymbol{I}_{N_m}\ \ H_{t_2}\boldsymbol{I}_{N_m} \ldots H_{t_{n_t+1}}\boldsymbol{I}_{N_m}]$$

$\boldsymbol{I}_{N_m}$ being an identity matrix of size N_m and $H_{t_1}, \ldots, H_{t_{n_t+1}}$ are the actual shape functions. For example, for $n_t = 3$,

$$H_{t_1} = -4.5s^3 + 9s^2 - 5.5s + 1, \quad H_{t_2} = 13.5s^3 - 22.5s^2 + 9s,$$

$$H_{t_3} = -13.5s^3 + 18s^2 - 4.5s, \quad H_{t_4} = 4.5s^3 - 4.5s^2 + s$$

Finally, Eqn. 4.3 becomes, for time element j,

$$\delta\boldsymbol{\xi}_j^T [-\dot{\boldsymbol{H}}_t^T \overline{\boldsymbol{M}} \dot{\boldsymbol{H}}_t + \boldsymbol{H}_t^T \overline{\boldsymbol{C}} \dot{\boldsymbol{H}}_t + \boldsymbol{H}_t^T \overline{\boldsymbol{K}} \boldsymbol{H}_t] \delta\boldsymbol{\xi}_j = \delta\boldsymbol{\xi}_j^T [\boldsymbol{H}_t^T \overline{\boldsymbol{F}}] \tag{4.4}$$

The elements are then assembled with the periodicity conditions in mind.

5 Load Calculations

The load calculations may be done by either the force summation or the modal curvature method.

5.1 Force Summation

Here, the blade aerodynamic and inertial loads are integrated spanwise to yield moments and shears at any section. The aerodynamic loads have already been estimated in Eqns. 3.10 and 3.11. Now that the blade response is known, the inertial loads are easily calculated :

$$F_I = -\iint_A \rho_S \bar{a}\, d\eta\, d\zeta \tag{5.1}$$

$$M_I = -\iint_A \bar{s} \rho_S \bar{a}\, d\eta\, d\zeta \tag{5.2}$$

Blade acceleration $\bar{a}$ and moment arm $\bar{s}$ are, respectively

$$\bar{a} = \ddot{\bar{r}} + \bar{\Omega} \times (\bar{\Omega} \times \bar{r}) + 2(\bar{\Omega} \times \dot{\bar{r}})$$

$$\bar{s} = -w^{0}(\eta \cos\theta_0)\hat{i} + (\eta \cos\theta_0 - \zeta \sin\theta_0)\hat{j} + (\eta \sin\theta_0 + \zeta \cos\theta_0)\hat{k}$$

$$\overline{\Omega} = \Omega \sin\beta_p \hat{i} + \Omega \cos\beta_p \hat{j}$$

Finally,

$$L_u^I = -m(-x + \beta_p w + 2\dot{\theta}_0 e_g \sin\theta_0) \qquad (5.3)$$

$$L_v^I = -m(-2\beta_p \dot{w} + e_g \cos\theta_0(-\dot{\theta}_0^2 - 2\beta_p \dot{\theta}_0 - 1 - \beta_p^2 - w'\theta_0') + e_g \sin\theta_0(-\ddot{\theta}_0 - 2\dot{w}')) \qquad (5.4)$$

$$L_w^I = -m(\ddot{w} + \beta_p x - \beta_p^2 w + e_g \cos\theta_0 \ddot{\theta} - \dot{\theta}_0^2 e_g \sin\theta_0) \qquad (5.5)$$

$$M_u^I = -m(K_m^2 \ddot{\theta}_0 + \cos\theta_0 \sin\theta_0 (K_{m2}^2 - K_{m1}^2)(1 - \beta_p w' + 2w'\dot{\theta}_0)$$
$$+2\dot{w}'(K_{m2}^2 \sin^2\theta_0 + K_{m1}^2 \cos^2\theta_0) + e_g \cos\theta_0(\ddot{w} + x\beta_p) + 2\beta_p \dot{w} e_g \sin\theta_0) \qquad (5.6)$$

$$M_v^I = -m(-2\dot{w}\theta_0' \cos\theta_0 \sin\theta_0 (K_{m2}^2 - K_{m1}^2) + (K_{m2}^2 \sin^2\theta_0 +$$
$$K_{m1}^2 \cos^2\theta_0)(w' - \ddot{w} + \beta_p + 2\dot{\theta}_0) + e_g \sin\theta_0(-x + \beta_p w + x\beta_p w')) \qquad (5.7)$$

$$M_w^I = -m(\cos\theta_0 \sin\theta_0 (K_{m2}^2 - K_{m1}^2)(\ddot{w}' - w'\dot{\theta}_0^2 - 2\dot{\theta}_0 - \beta_p - w')$$
$$+(K_{m1}^2 \sin^2\theta_0 + K_{m2}^2 \cos^2\theta_0)(2\dot{w}'\dot{\theta}_0 + w'\ddot{\theta}_0) + e_g \cos\theta_0(x - \beta_p w)) \qquad (5.8)$$

e_g is the offset of blade c.g.ahead of the elastic axis.K_{m1}^2, K_{m2}^2 are flapwise and chordwise moments of inertia per unit blade length.Formally,

$$me_g = \iint_A \rho_S \eta \, d\eta \, d\zeta \,, \quad mK_{m1}^2 = \iint_A \rho_S \zeta^2 \, d\eta \, d\zeta \,, \quad mK_{m2}^2 = \iint_A \rho_S \eta^2 \, d\eta \, d\zeta$$

The acceleration $\ddot{w}$ is got from the equation of motion Eqn. 3.18 using the displacements, velocities and the known matrices.

The rotating frame hub loads are got by integrating these sectional blade loads across the blade :

$$\begin{Bmatrix} F_x \\ F_y \\ F_z \end{Bmatrix} = \int_0^R \begin{Bmatrix} L_u \\ L_v \\ L_w \end{Bmatrix} dx \tag{5.9}$$

$$\begin{Bmatrix} M_x \\ M_y \\ M_z \end{Bmatrix} = \int_0^R \begin{Bmatrix} -L_v w + M_u \\ L_u w - L_w x + M_v \\ L_v x + M_w \end{Bmatrix} dx \tag{5.10}$$

5.2 Modal Method

The blade response is directly differentiated to determine the loads in this method. It is inaccurate as compared to the more detailed force summation method, but for this simplified problem, it yields identical results.

The flap, lag and torsional bending moments are given by

$$M_\eta = \iint_A \zeta\sigma d\eta d\zeta = EI_\eta[-w''\cos\theta_0]$$

$$M_\zeta = -\iint_A \eta\sigma d\eta d\zeta = EI_\zeta[-w''\sin\theta_0]$$

$$\begin{aligned} M_\xi &= \iint_A [\eta\sigma_{x\zeta} - \zeta\sigma_{x\eta} + \lambda_T(\frac{\partial\sigma_{x\zeta}}{\partial\zeta} + \frac{\partial\sigma_{x\eta}}{\partial\eta})]d\eta d\zeta \\ &+ \frac{\partial}{\partial x}\iint_A \lambda_T\sigma_{xx}\, d\eta d\zeta + \theta_0' \iint_A (\eta^2 + \zeta^2)\sigma_{xx}\, d\eta d\zeta \\ &= -EB_2\theta_0' w''\sin\theta_0 \end{aligned}$$

with

$$EB_2 = \iint_A \eta(\eta^2 + \zeta^2)^2 d\eta d\zeta$$

5.3 Hub Loads

The fixed frame hub loads are (assuming one of the blades is located at ψ)

$$F_x^H(\psi) = \sum_{m=1}^{N_b} (F_x^m \cos\psi_m - F_y^m \sin\psi_m - F_z^m \cos\psi_m \beta_p) \tag{5.11}$$

$$F_y^H(\psi) = \sum_{m=1}^{N_b} (F_x^m \sin\psi_m + F_y^m \cos\psi_m - F_z^m \sin\psi_m \beta_p) \tag{5.12}$$

$$F_z^H(\psi) = \sum_{m=1}^{N_b} (F_z^m + F_x^m \beta_p) \tag{5.13}$$

$$M_x^H(\psi) = \sum_{m=1}^{N_b} (M_x^m \cos\psi_m - M_y^m \sin\psi_m - M_z^m \cos\psi_m \beta_p) \tag{5.14}$$

$$M_y^H(\psi) = \sum_{m=1}^{N_b} (M_x^m \sin\psi_m + M_y^m \cos\psi_m - M_z^m \sin\psi_m \beta_p) \tag{5.15}$$

$$M_z^H(\psi) = \sum_{m=1}^{N_b} (M_z^m + M_x^m \beta_p) \tag{5.16}$$

This summation only transmits harmonics which are integral multiples of N_b. Thus the hub loads have a large N_b/rev component. The steady part of these loads are represented as H, Y, T, M_x, M_y, M_z (eg. $T = \int_0^{2\pi} F_z^H(\psi)d\psi$)

6 Jacobian and Controls Update

The 6 nonlinear trim equations Eqns. 1.1 through 1.6 are linearized using a Taylor series expansion about the current controlstate to obtain trim condition at the updated state i.e.

$$F(\theta_i + \Delta\theta_i) = F(\theta_i) + \frac{\partial F}{\partial \theta_i}\Big|_{\theta=\theta_i} \Delta\theta_i = 0$$

F is the vector of residuals in the 6 trim equations. Thus

$$\Delta\theta_i = -\frac{\partial F}{\partial \theta}^{-1} F(\theta_i)$$

The update happens as

$$\theta_{i+1} = \theta_i + \Delta\theta_i$$

To calculate the Trim Jacobian $\partial F/\partial\theta$, a simple forward difference approximation is used by calculating the residuals before and after a slight perturbation in each control variable.

$$\frac{\partial F}{\partial \theta} \sim \frac{F(\theta + \Delta\theta) - F(\theta)}{\Delta\theta}$$

When the norm of the residuals and control updates reach a specified tolerance, the analysis is stopped.

Note that in this case, there are only 4 control variables that are fed into the analysis, namely θ_0 (collective pitch), θ_{1c}, θ_{1s} and λ. The shaft inclinations are outputs of the trimming procedure. As a result, only 4 residuals need to be monitored. It can be seen, for instance, that the side force equation is not as critical as the rest.

7 Results

The results were calculated for a rotor with the following properties :

- $C_w/\sigma = 0.07$
- $\sigma = 0.085$
- $c/R = 0.05$
- $\beta_p, \theta_{tw} = 0$
- $N_b = 4$
- Lock Number $\gamma = 8$
- $x_{cg}, y_{cg} = 0$

• h/R = 0.2

• Airfoil properties : C_l = 5.7; C_d = 0.01; c_{mac}, e_g, e_d, f_1 = 0

• EI_z = 0; EI_y = 0.0108

• First flapping frequency is caculated to be ν_β = 1.126/rev

The results have been compiled for an advance ratio μ = 0.3.10 finite elements in space and 12 finite elements in time (of order 5) were used.

Fig. 2 shows that the maximum flapping occurs on the retreating side while minimum flapping occurs on the advancing side. This is consistent with the fact that as the flapping occurs at a frequency close to 1/rev, the flapping response lags about a quarter cycle (90°) behind the loads.

Fig. 3 shows that with lower advance ratios, the displacements become more uniform, since the asymmetry between loads on the advancing and retreating blades becomes smaller.

Fig. 4 and 7 through 12 show that the steady hub loads (for N_b = 4) are primarily 4/rev in nature.

Fig. 5 and 13 through 18 show that the aerodynamic contributions are largely to the vertical shear and flapping moment.

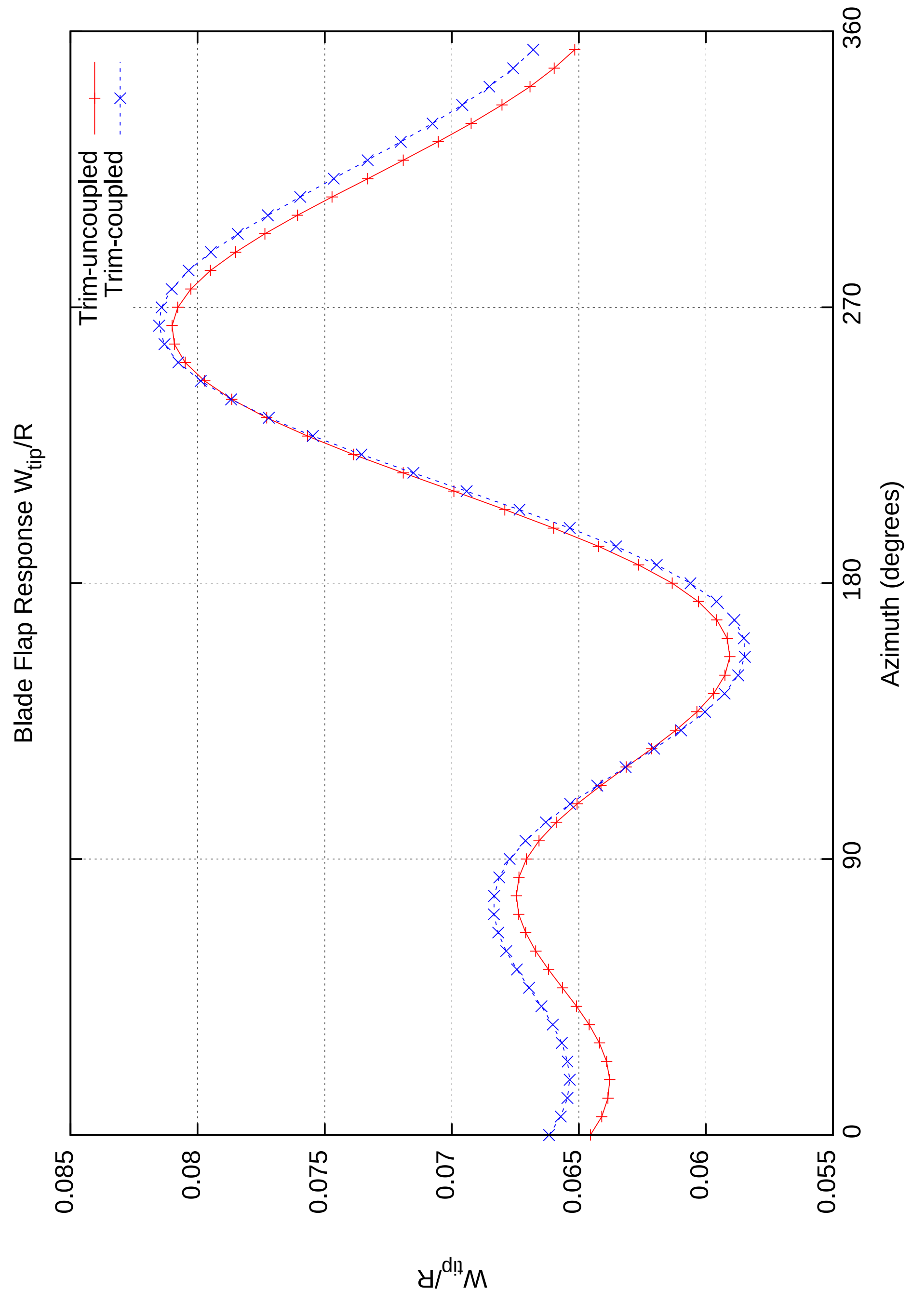
Blade Flap Response W_{tip}/R
Trim-uncoupled
Trim-coupled
Azimuth (degrees)
W_{tip}/R
0
90
180
270
360
0.055
0.06
0.065
0.07
0.075
0.08
0.085

Figure 2:

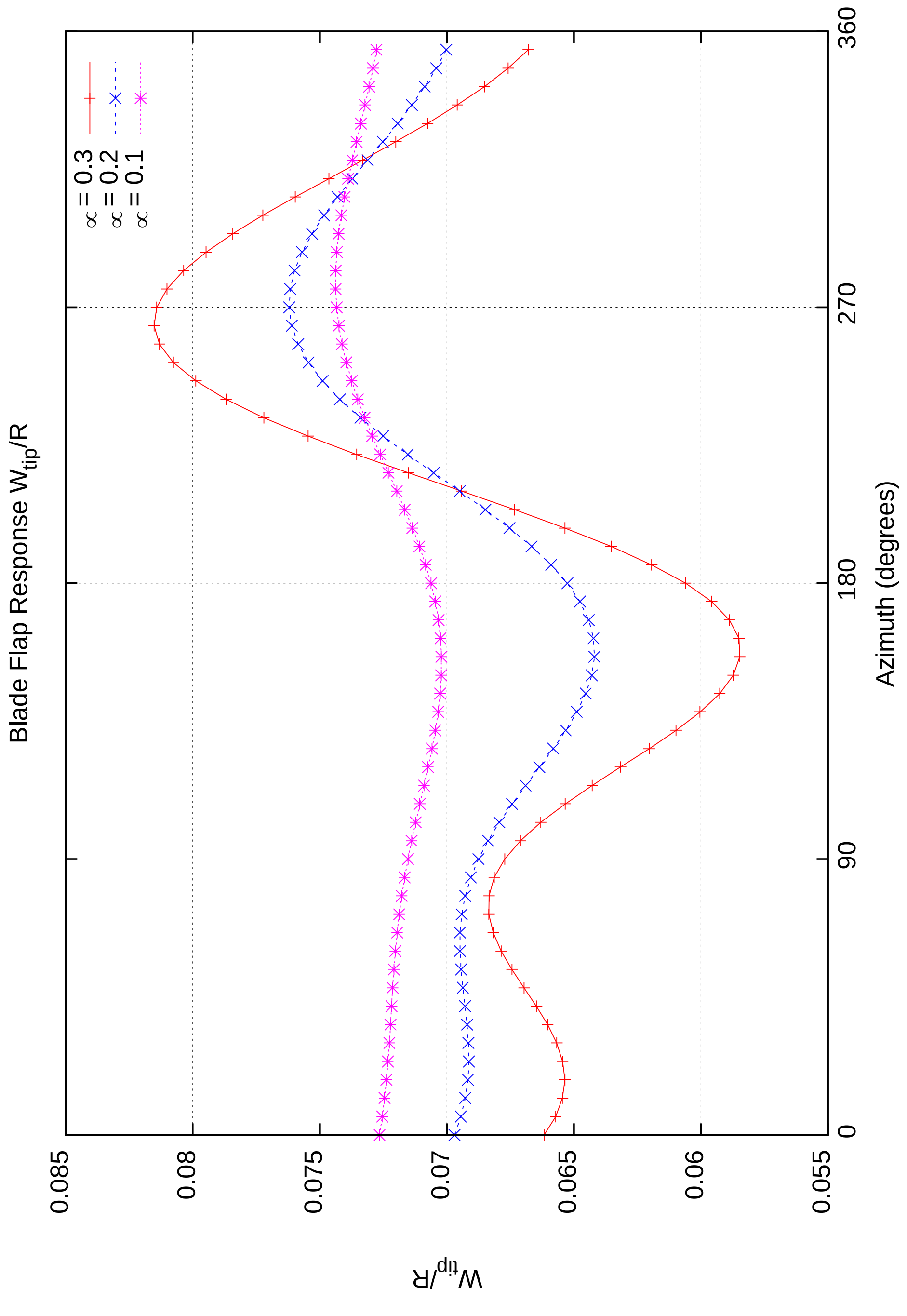
Blade Flap Response W_{tip}/R
W_{tip}/R
Azimuth (degrees)
$\propto = 0.3$
$\propto = 0.2$
$\propto = 0.1$
0.085
0.08
0.075
0.07
0.065
0.06
0.055
0
90
180
270
360

Figure 3:

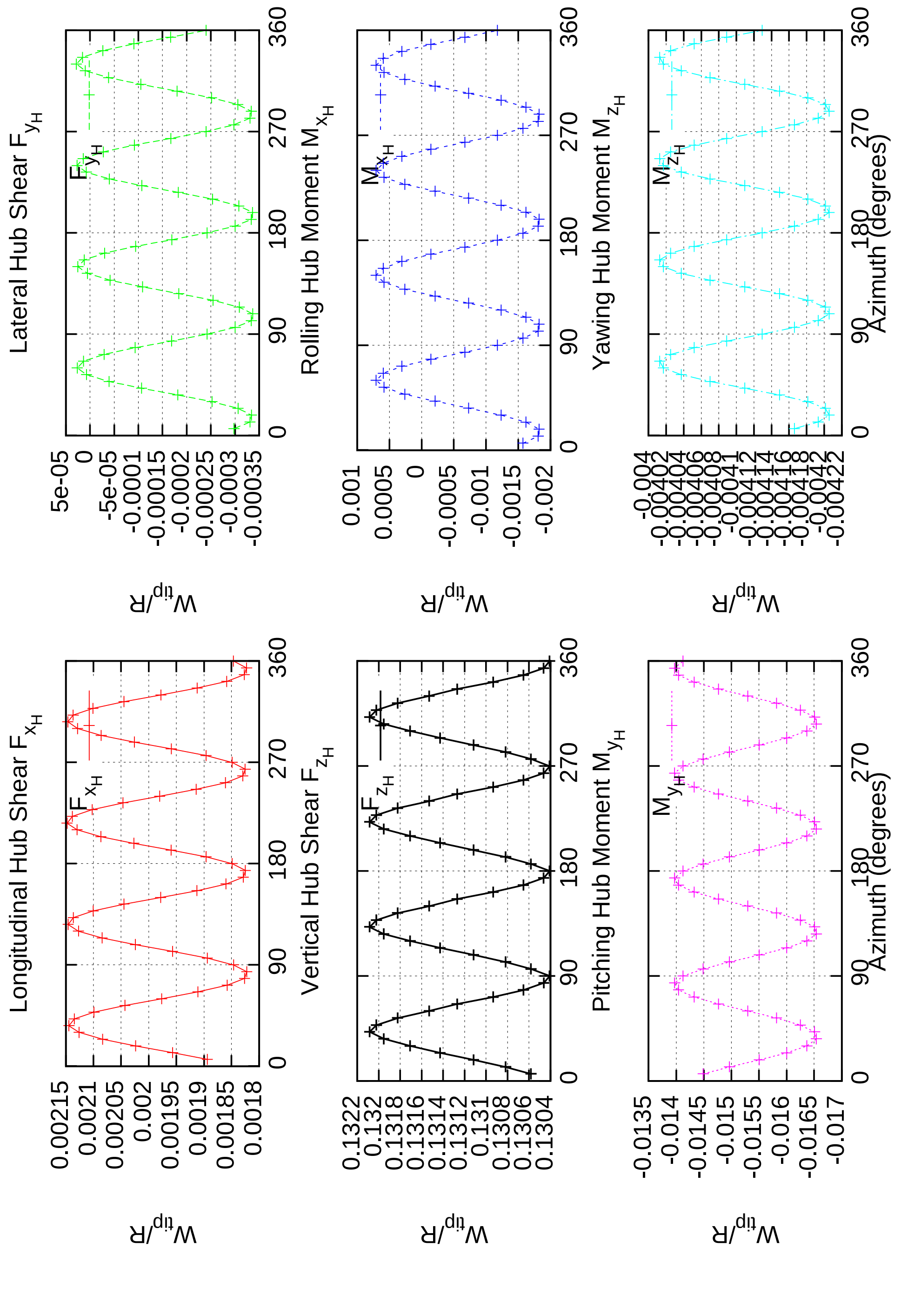
Longitudinal Hub Shear F_{x_H}
Lateral Hub Shear F_{y_H}
Vertical Hub Shear F_{z_H}
Rolling Hub Moment M_{x_H}
Pitching Hub Moment M_{y_H}
Yawing Hub Moment M_{z_H}
W_{tip}/R
Azimuth (degrees)

Figure 4:

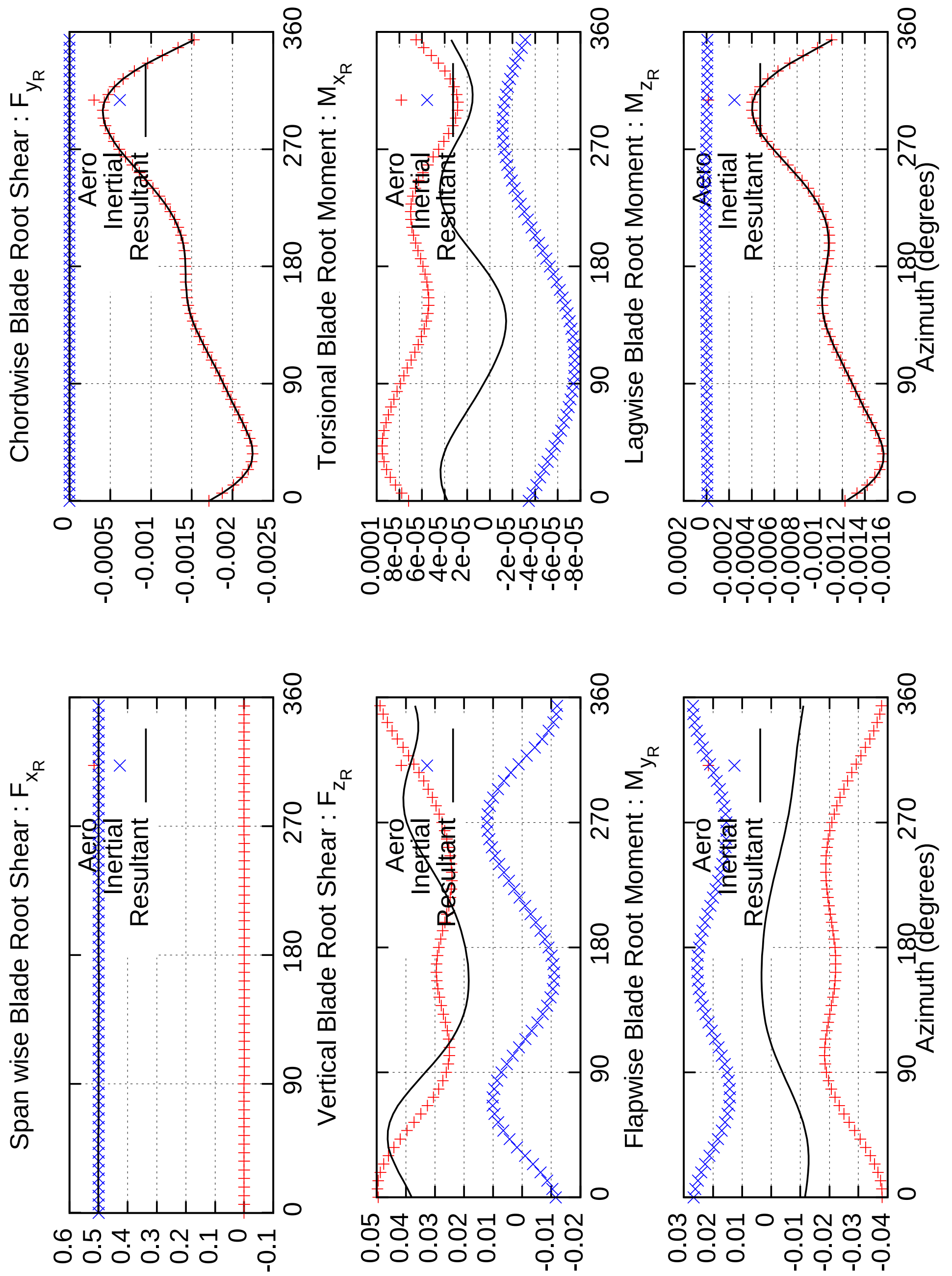

Span wise Blade Root Shear : F_{x_R}
Chordwise Blade Root Shear : F_{y_R}
Vertical Blade Root Shear : F_{z_R}
Torsional Blade Root Moment : M_{x_R}
Flapwise Blade Root Moment : M_{y_R}
Lagwise Blade Root Moment : M_{z_R}
Aero
Inertial
Resultant
Azimuth (degrees)

Figure 5:

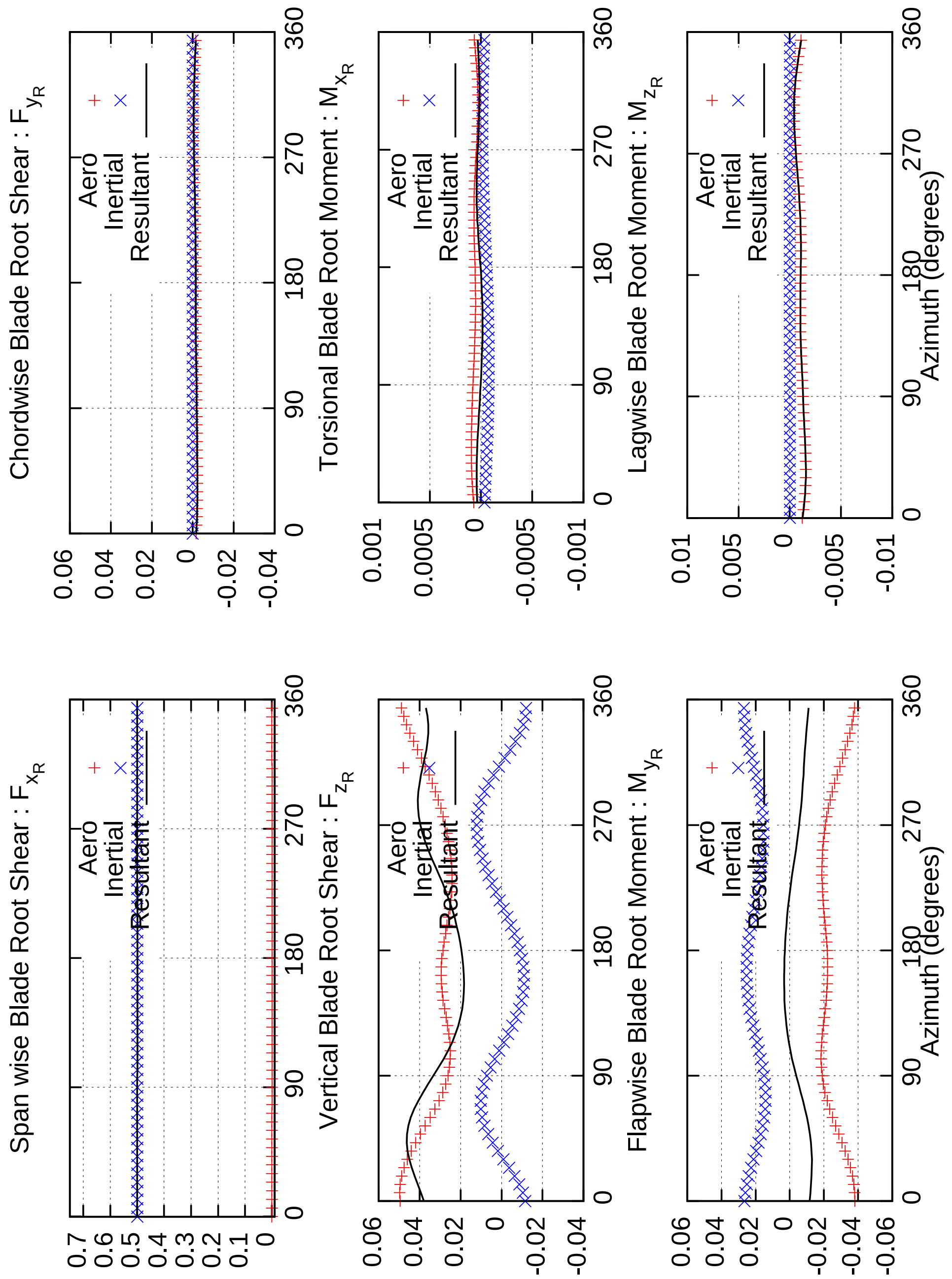

Span wise Blade Root Shear : F_{x_R}
Chordwise Blade Root Shear : F_{y_R}
Vertical Blade Root Shear : F_{z_R}
Torsional Blade Root Moment : M_{x_R}
Flapwise Blade Root Moment : M_{y_R}
Lagwise Blade Root Moment : M_{z_R}
Aero
Inertial
Resultant
Azimuth (degrees)

Figure 6:

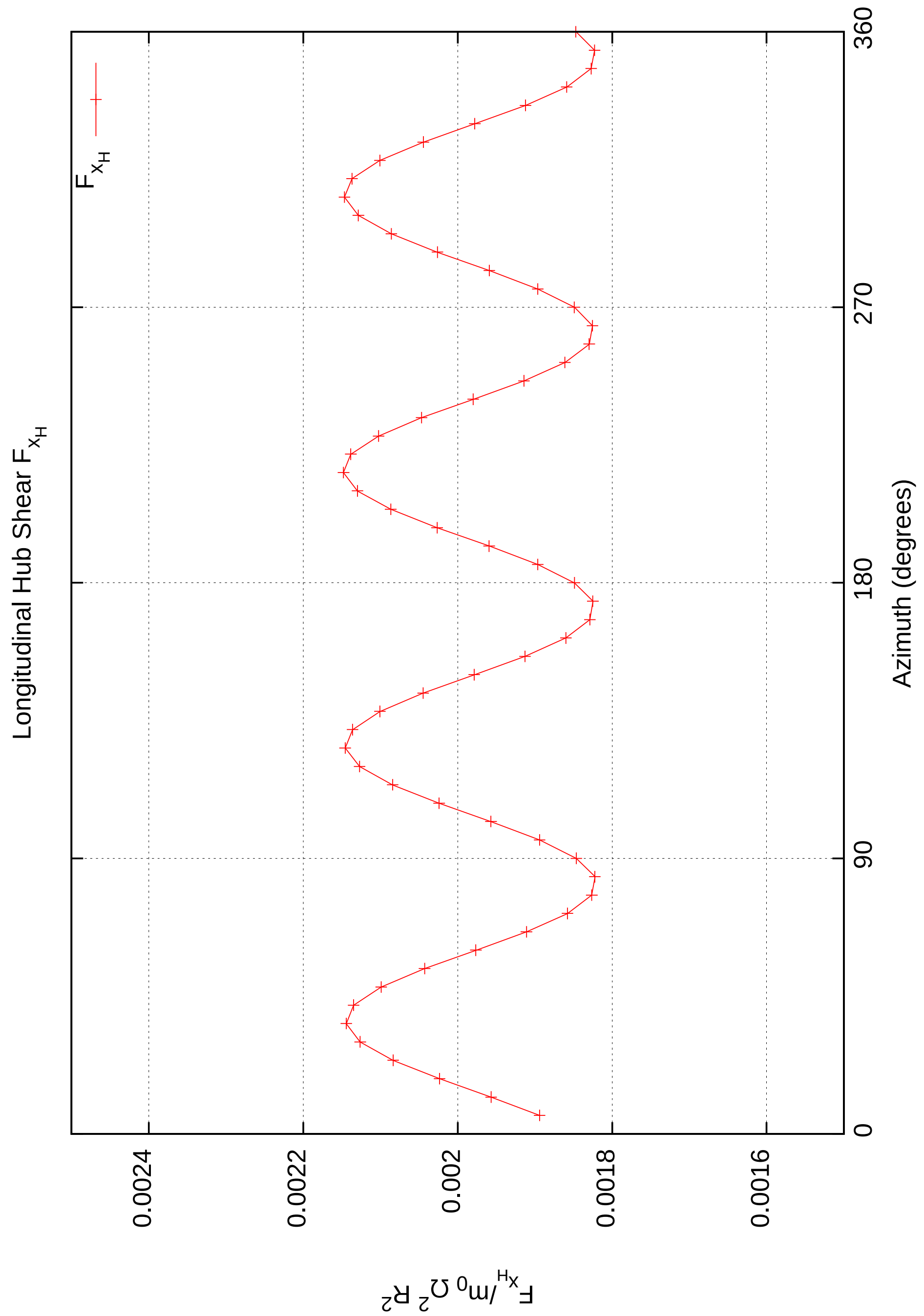

Longitudinal Hub Shear F_{x_H}
F_{x_H}
$F_{x_H}/m_0\,\Omega^2\,R^2$
0.0024
0.0022
0.002
0.0018
0.0016
0
90
180
270
360
Azimuth (degrees)

Figure 7:

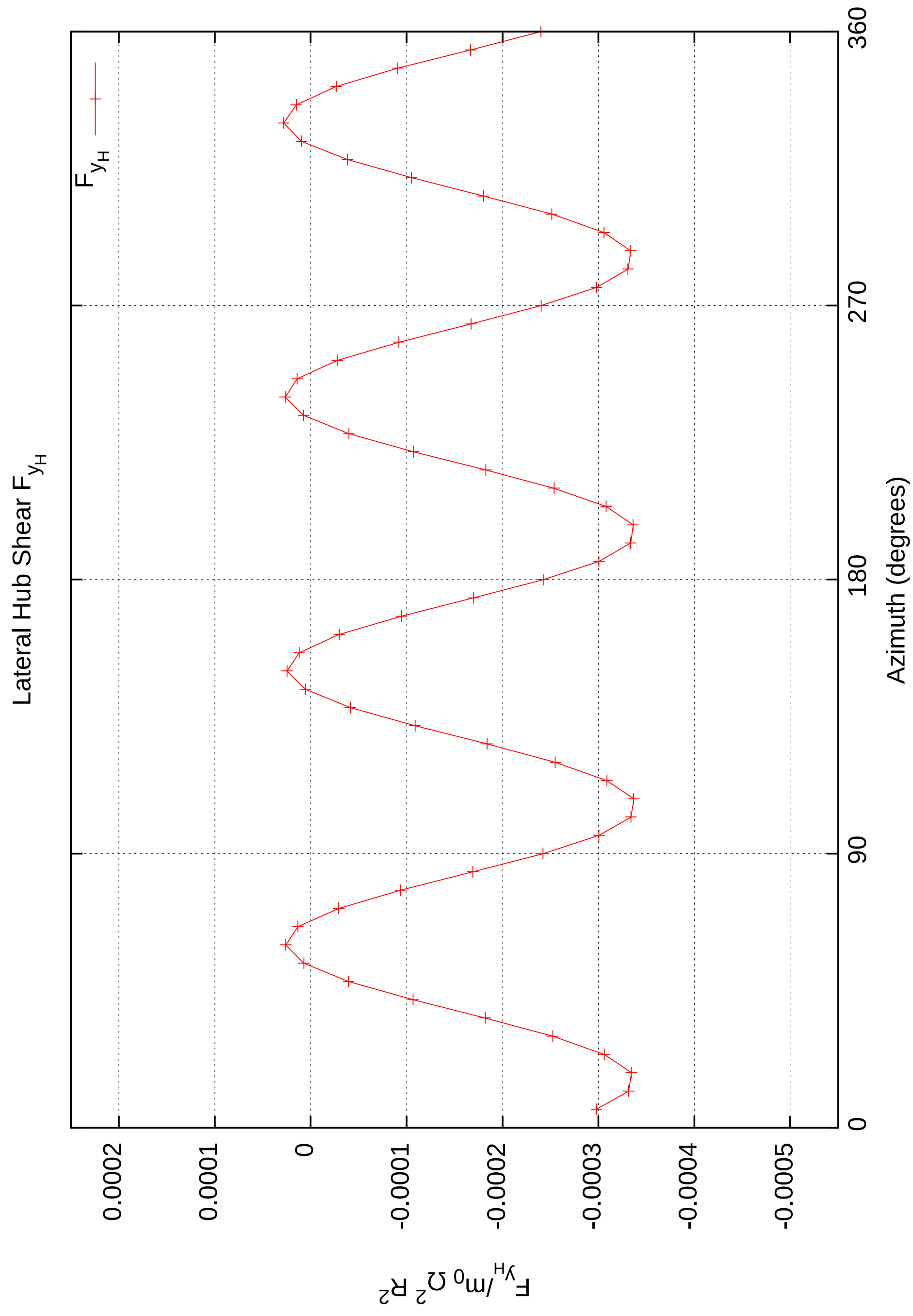
Lateral Hub Shear F_{y_H}
F_{y_H}
Azimuth (degrees)
0
90
180
270
360
$F_{y_H}/m_0\ \Omega^2\ R^2$
0.0002
0.0001
0
-0.0001
-0.0002
-0.0003
-0.0004
-0.0005

Figure 8:

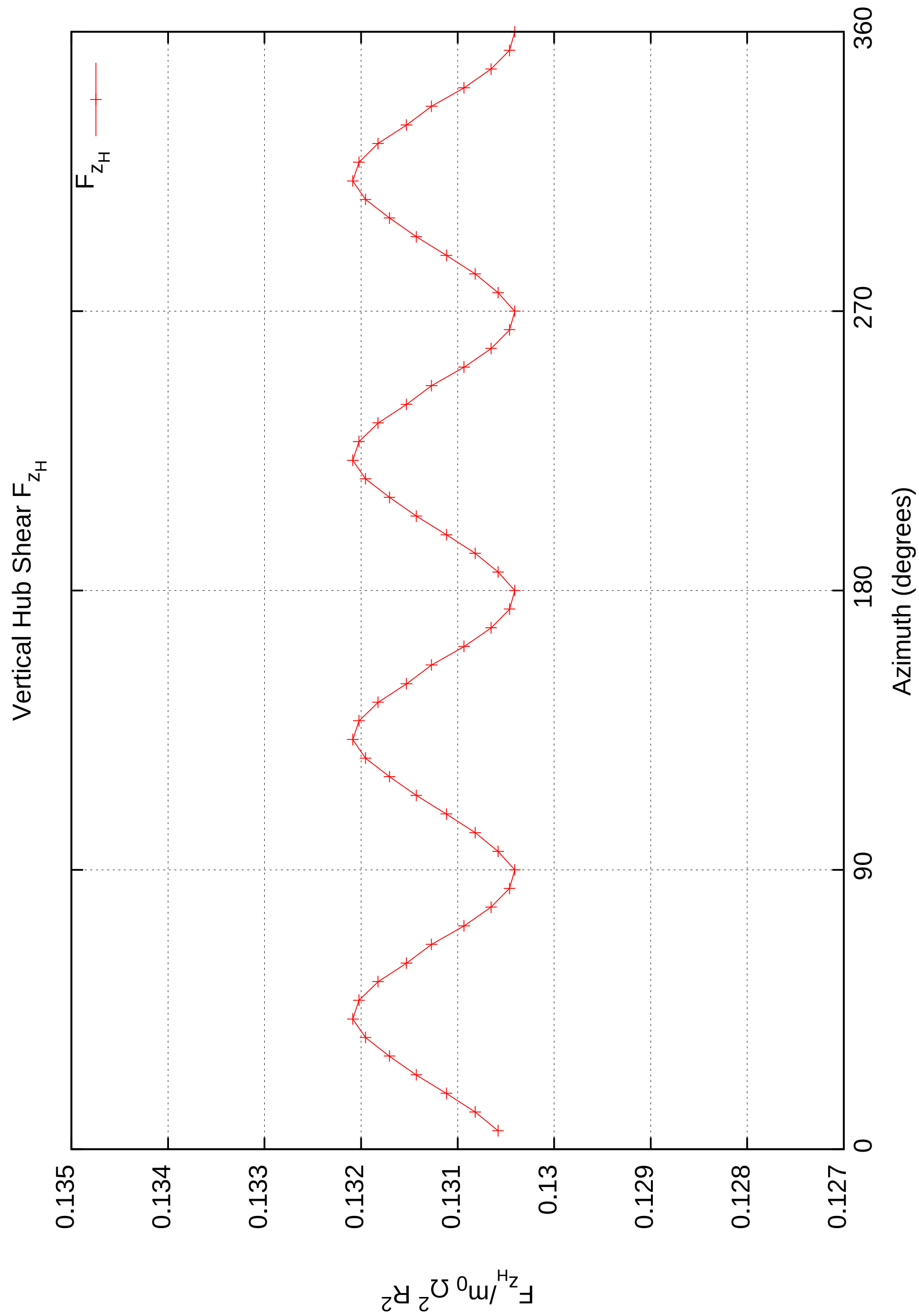
Vertical Hub Shear F_{z_H}
F_{z_H}
$F_{z_H}/m_0\,\Omega^2 R^2$
Azimuth (degrees)
0.135
0.134
0.133
0.132
0.131
0.13
0.129
0.128
0.127
0
90
180
270
360

Figure 9:

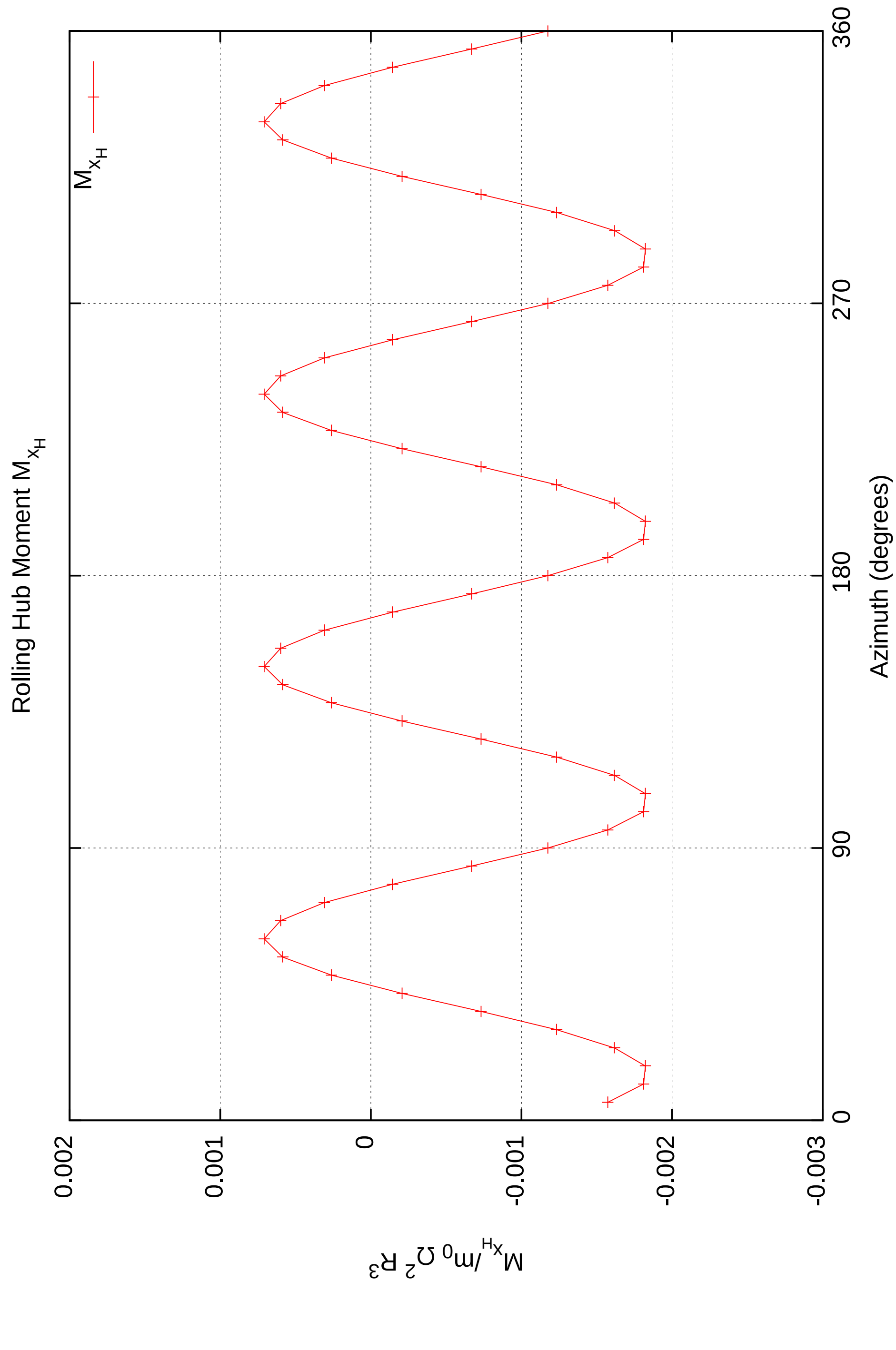
Rolling Hub Moment M_{x_H}
M_{x_H}
$M_{x_H}/m_0\,\Omega^2 R^3$
Azimuth (degrees)
0.002
0.001
0
-0.001
-0.002
-0.003
0
90
180
270
360

Figure 10:

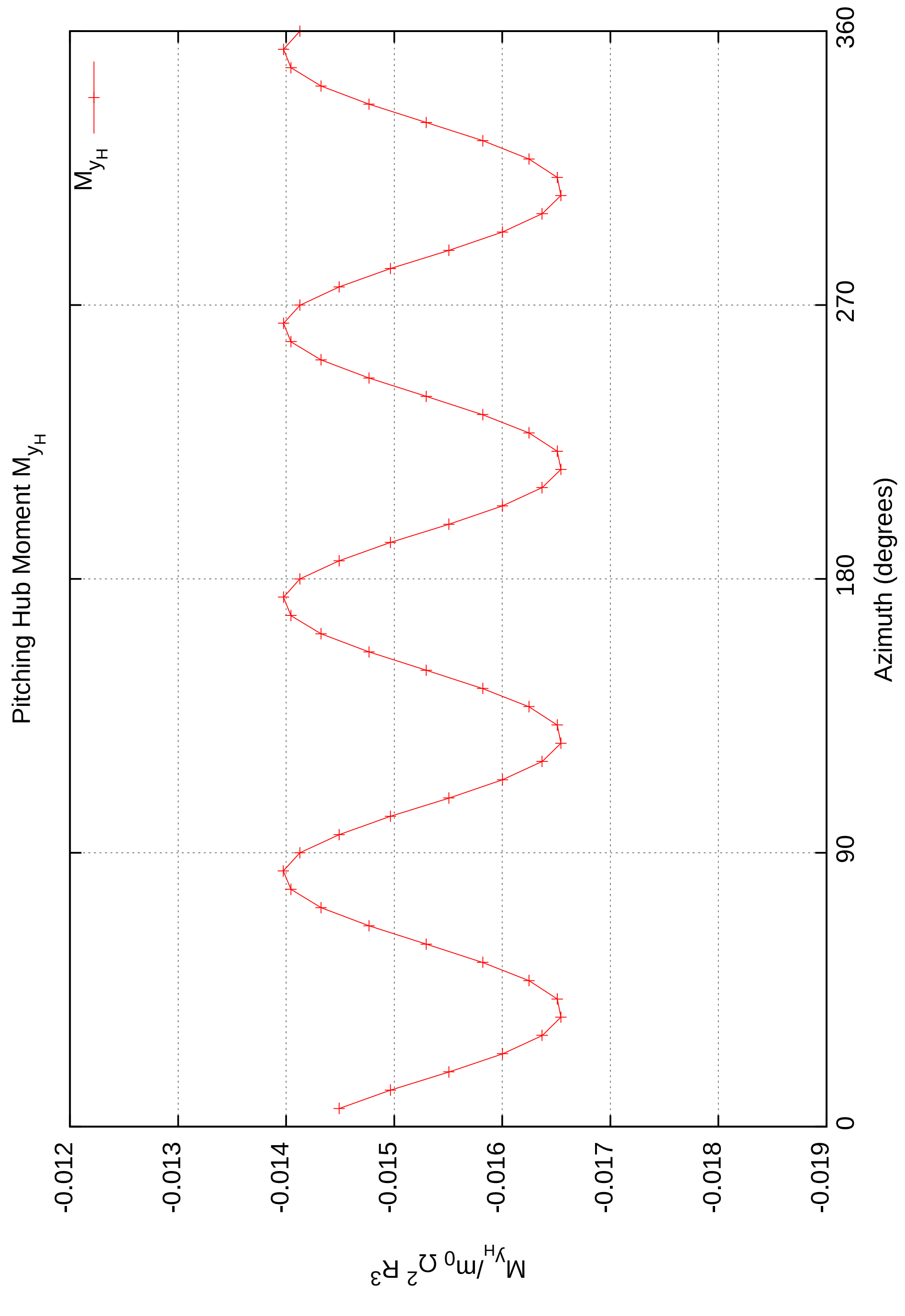
Pitching Hub Moment M_{y_H}
M_{y_H}
Azimuth (degrees)
$M_{y_H}/m_0\,\Omega^2\,R^3$
0
90
180
270
360
-0.012
-0.013
-0.014
-0.015
-0.016
-0.017
-0.018
-0.019

Figure 11:

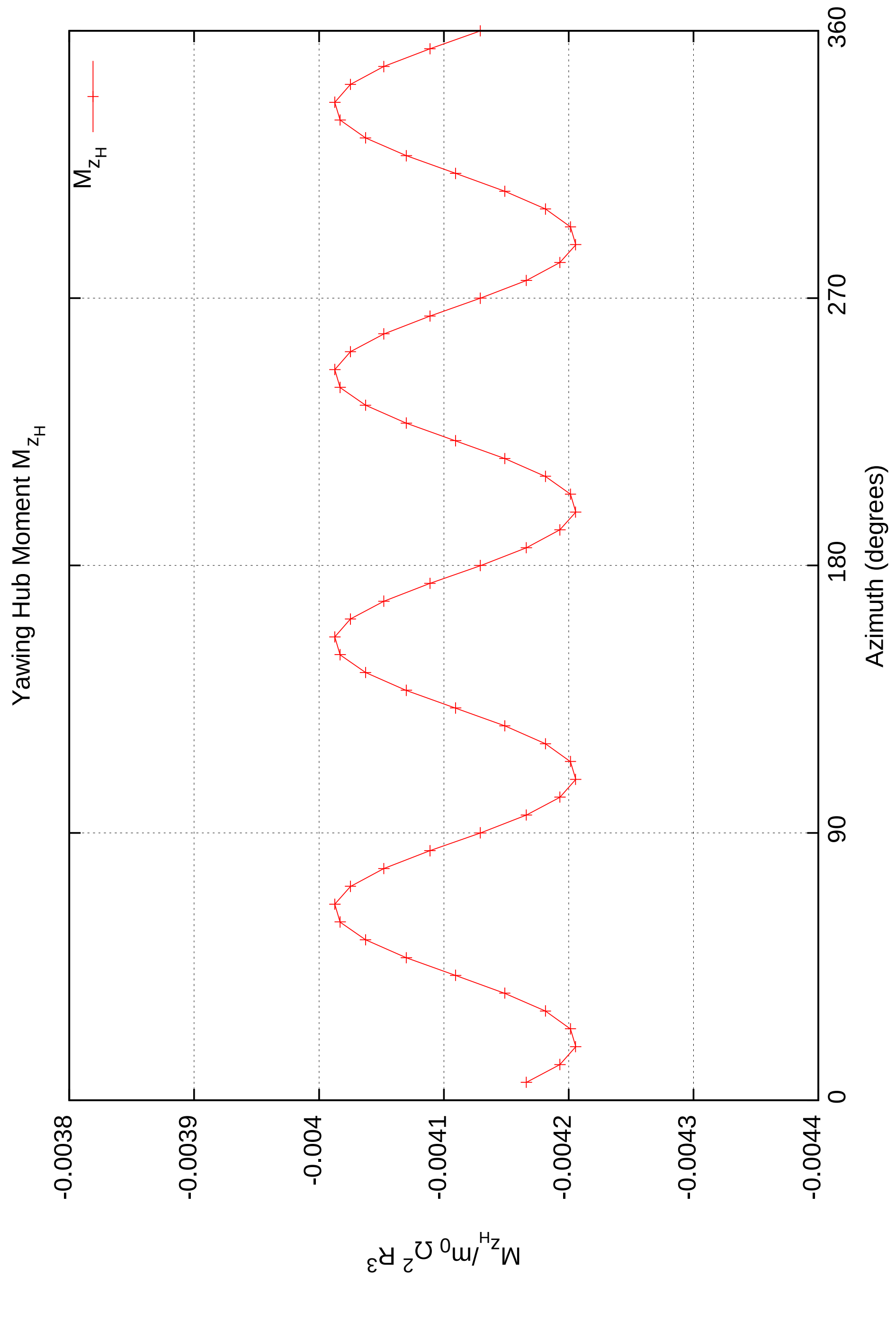

Yawing Hub Moment M_{z_H}
M_{z_H}
-0.0038
-0.0039
-0.004
-0.0041
-0.0042
-0.0043
-0.0044
$M_{z_H}/m_0\,\Omega^2\,R^3$
0
90
180
270
360
Azimuth (degrees)

Figure 12:

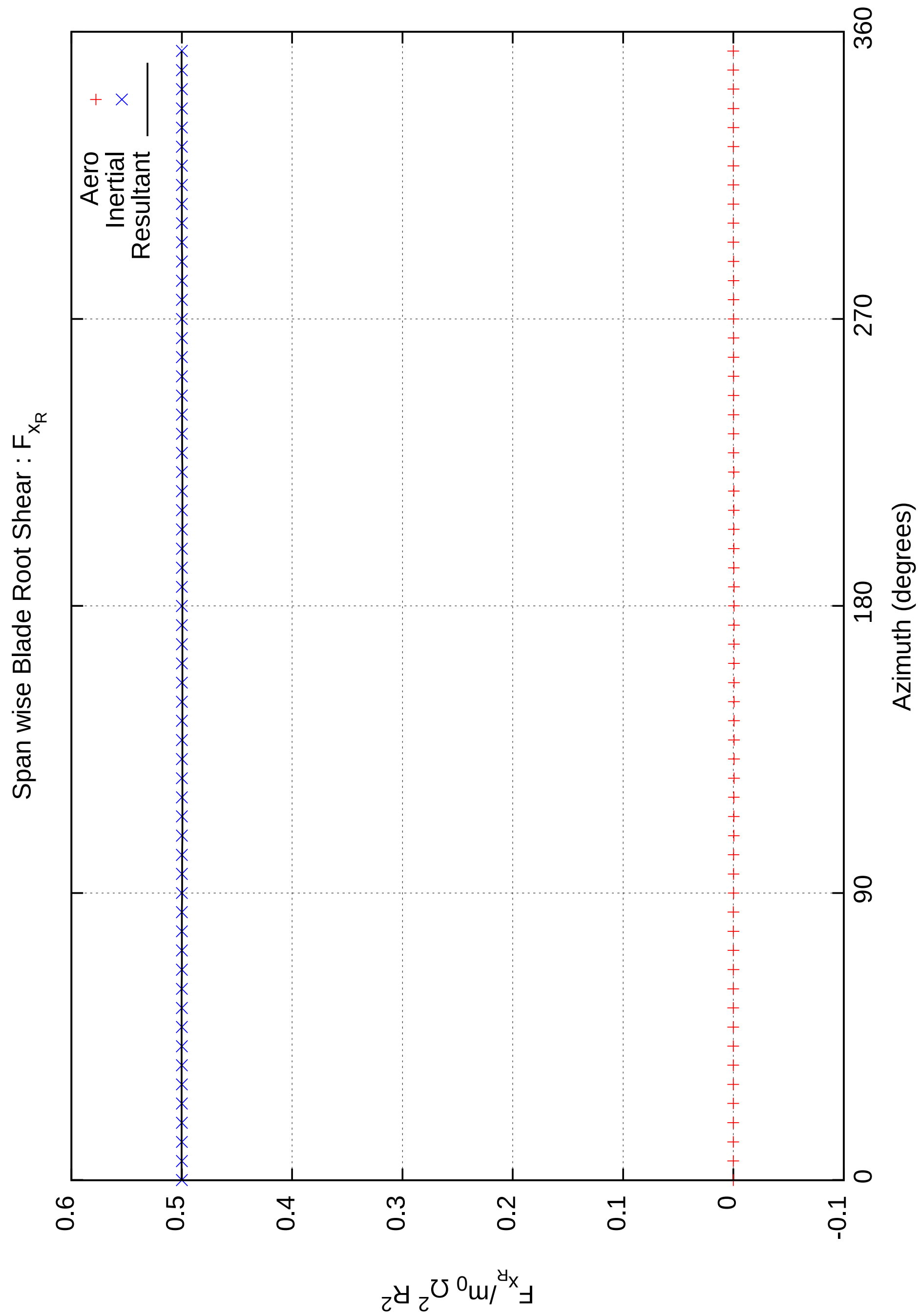
Span wise Blade Root Shear : F_{x_R}
Aero
Inertial
Resultant
Azimuth (degrees)
$F_{x_R}/m_0\,\Omega^2\,R^2$
0
90
180
270
360
0.6
0.5
0.4
0.3
0.2
0.1
0
-0.1

Figure 13:

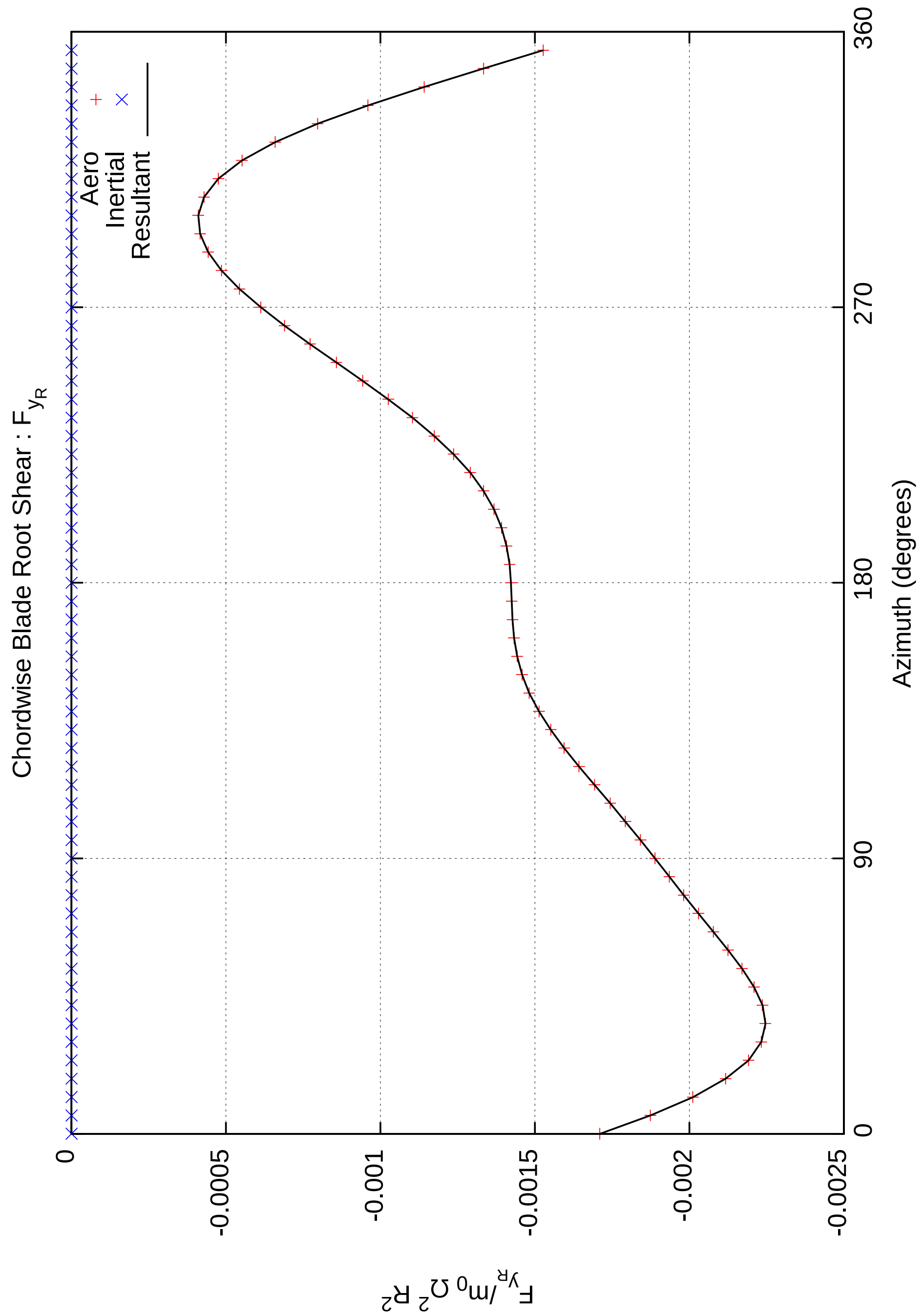
Chordwise Blade Root Shear : F_{y_R}
$F_{y_R}/m_0\,\Omega^2\,R^2$
Azimuth (degrees)
Aero
Inertial
Resultant
0
-0.0005
-0.001
-0.0015
-0.002
-0.0025
0
90
180
270
360

Figure 14:

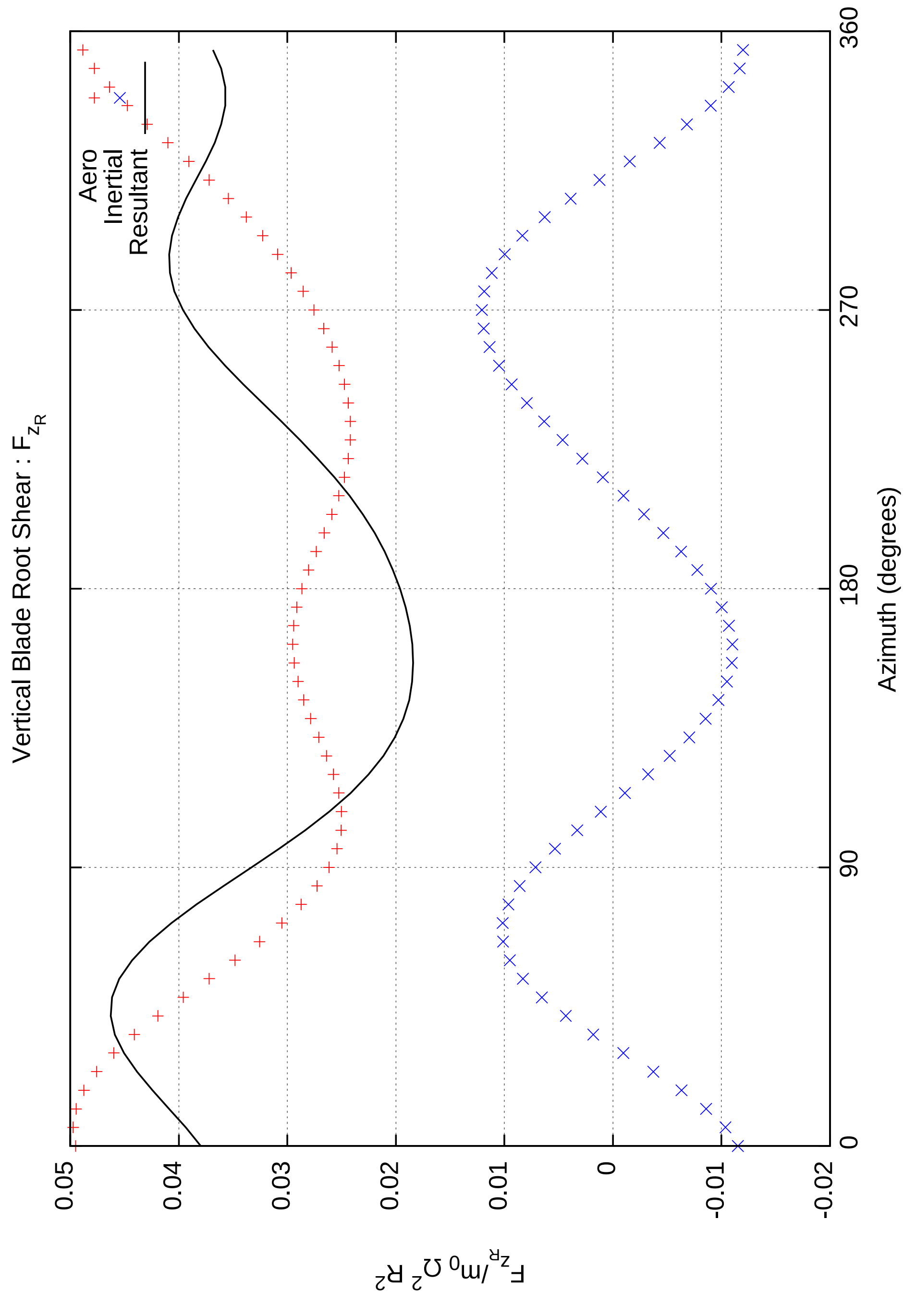
Vertical Blade Root Shear : F_{z_R}
Aero
Inertial
Resultant
$F_{z_R}/m_0\ \Omega^2\ R^2$
Azimuth (degrees)
0.05
0.04
0.03
0.02
0.01
0
-0.01
-0.02
0
90
180
270
360

Figure 15:

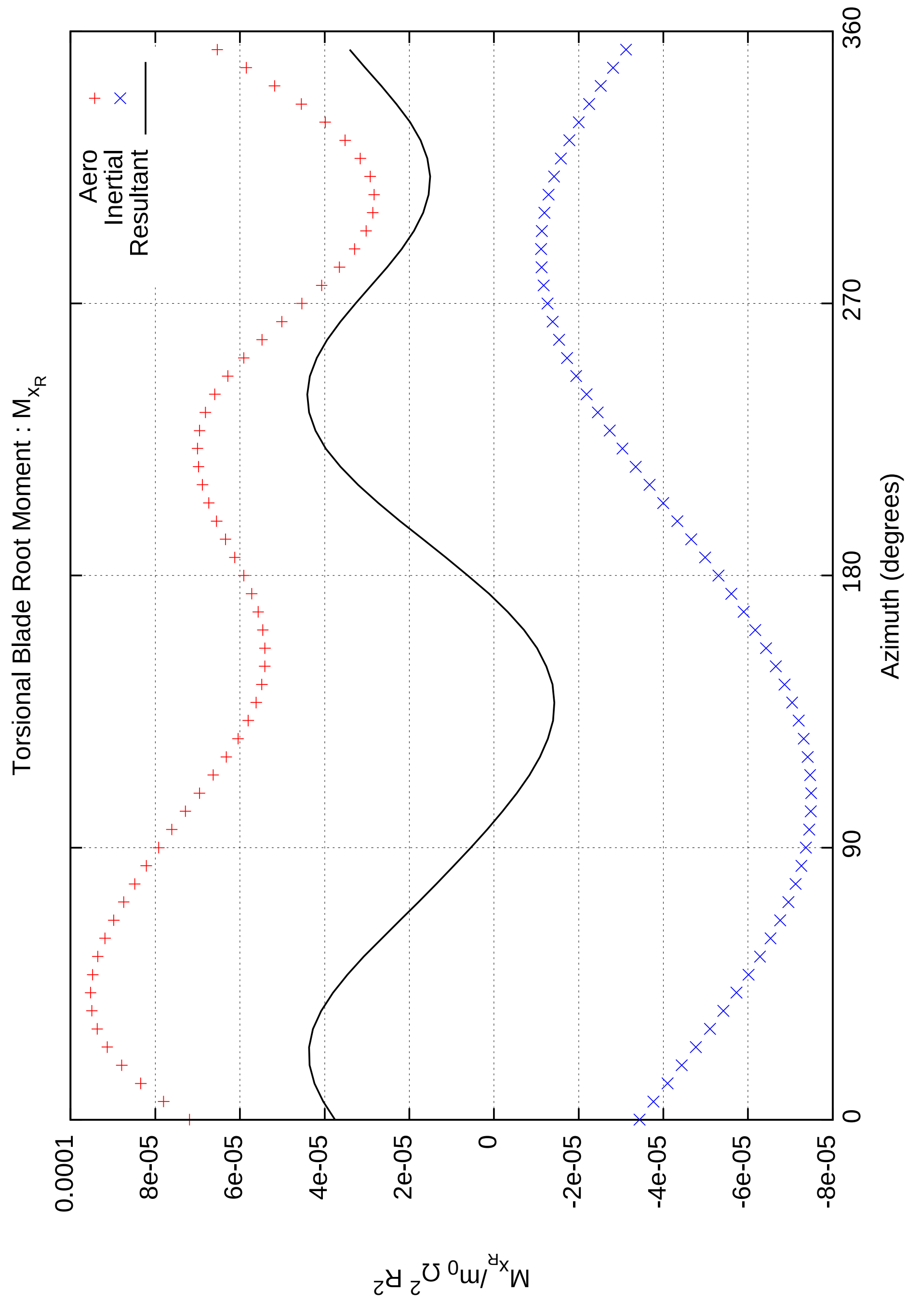
Torsional Blade Root Moment : M_{x_R}
Aero
Inertial
Resultant
$M_{x_R}/m_0\,\Omega^2\,R^2$
Azimuth (degrees)
0.0001
8e-05
6e-05
4e-05
2e-05
0
-2e-05
-4e-05
-6e-05
-8e-05
0
90
180
270
360

Figure 16:

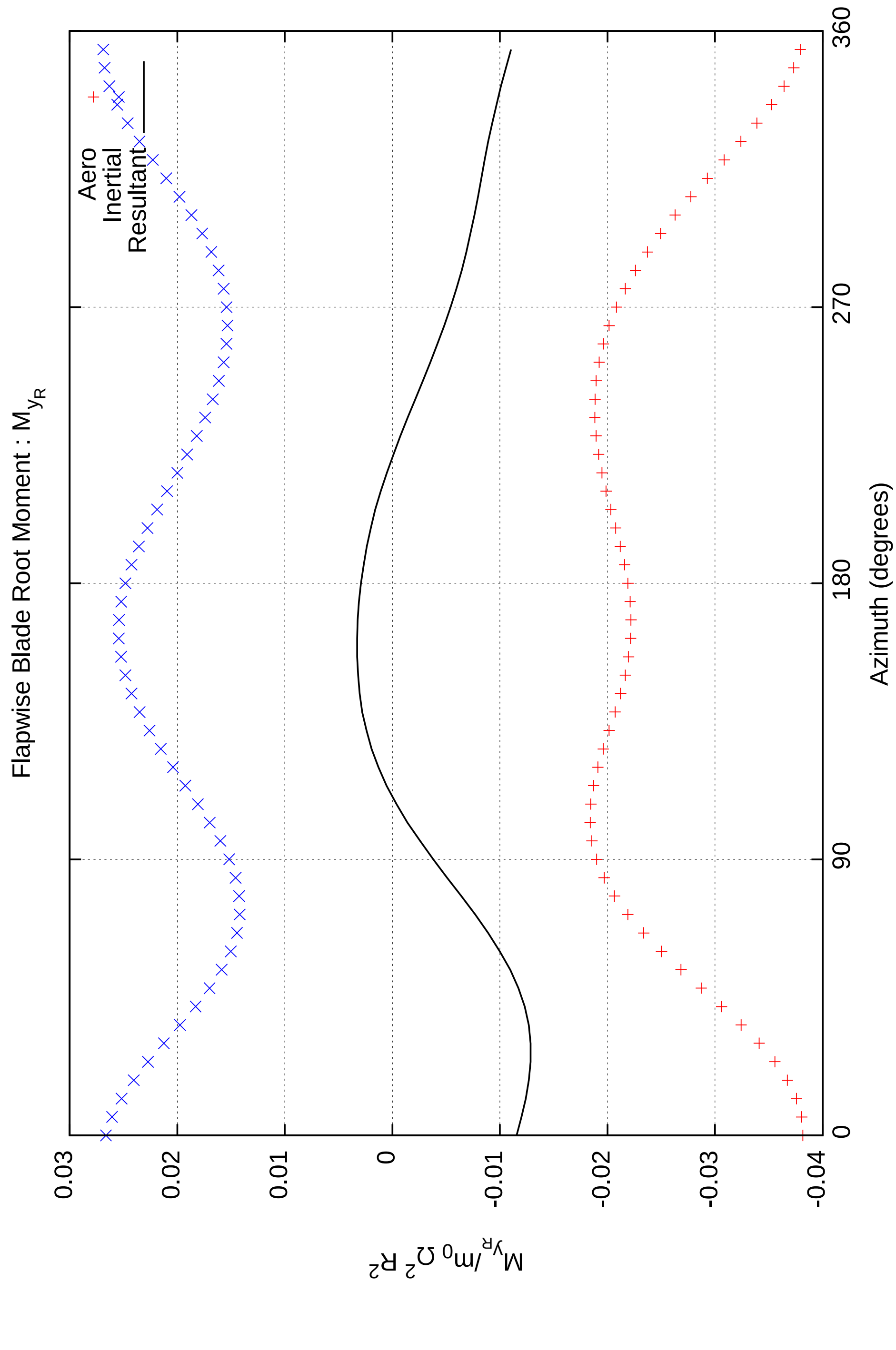
Flapwise Blade Root Moment : M_{y_R}
Aero
Inertial
Resultant
$M_{y_R}/m_0\,\Omega^2\,R^2$
Azimuth (degrees)
0.03
0.02
0.01
0
-0.01
-0.02
-0.03
-0.04
0
90
180
270
360

Figure 17:

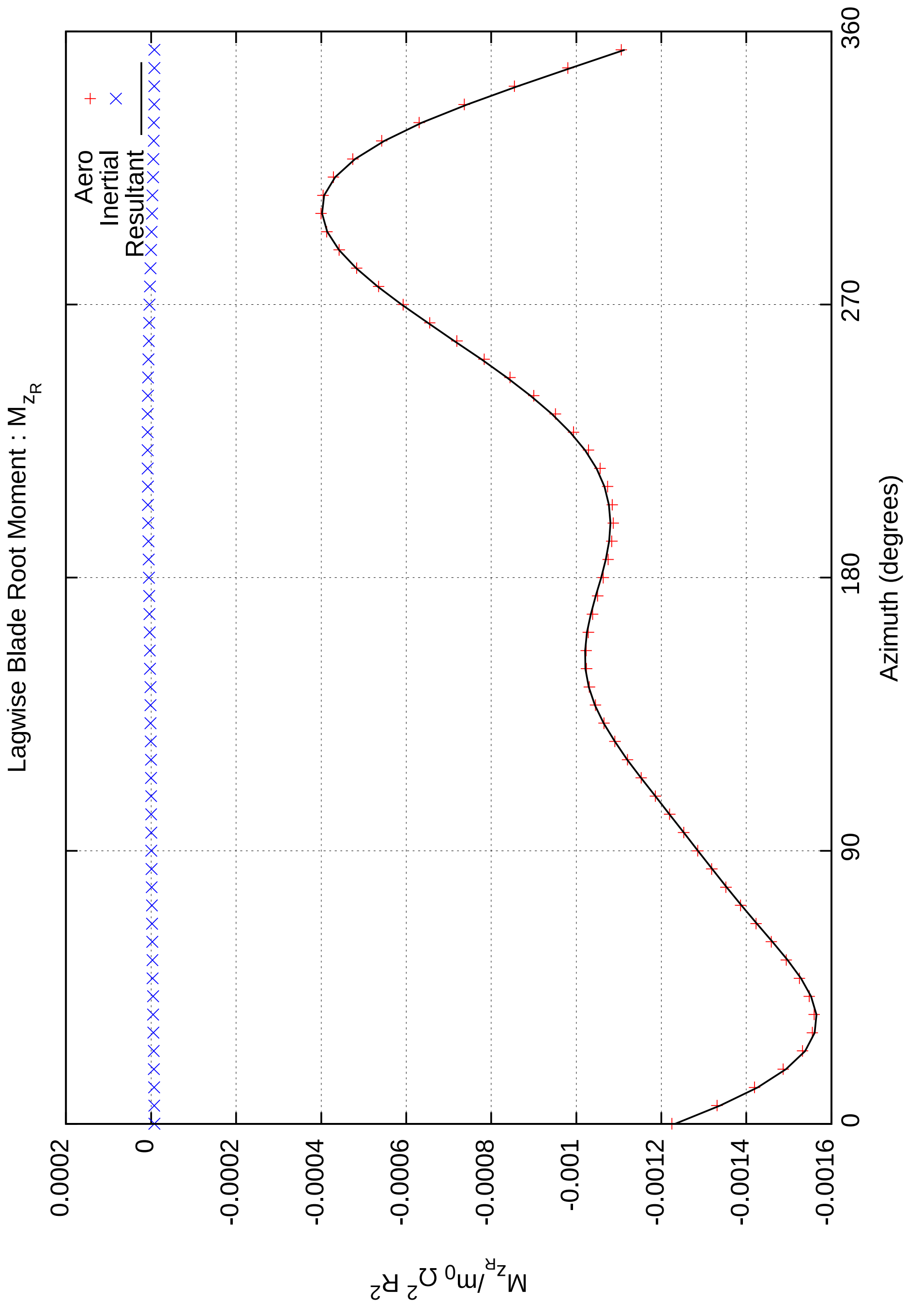
Lagwise Blade Root Moment : M_{z_R}
Aero
Inertial
Resultant
Azimuth (degrees)
$M_{z_R}/m_0\ \Omega^2\ R^2$
0
90
180
270
360
0.0002
0
-0.0002
-0.0004
-0.0006
-0.0008
-0.001
-0.0012
-0.0014
-0.0016

Figure 18: